SAW Front-End Module for GSM-Based Dual-Band Cellular Phones With Direct-Conversion Demodulation

Mitsutaka Hikita, *Fellow, IEEE*, Naoki Matsuura, Kazuyuki Yokoyama, Nobuhiko Shibagaki, and Kazuyuki Sakiyama

***Abstract*—Assuming direct-conversion (DC) demodulation, the required characteristics for surface-acoustic-wave (SAW) front-end modules (FEMs) have been investigated. A new FEM configuration is described that consists of not only transmitter (Tx) switching p-i-n diodes and a diplexer with low-pass/high-pass filters, but also SAW filters and baluns. A direct parallel connection between a SAW filter and a p-i-n diode makes it possible to drastically reduce the number of circuit elements. A module developed for an extended global system for mobile communications (EGSM)/digital cellular system (DCS) dual-band cellular-phone transceiver achieved insertion losses in the receiver (Rx) portions as small as 3.0 and 3.3 dB for EGSM and DCS, respectively. The Rx portions had attenuation characteristics as high as 30–40 dB at harmonic frequencies up to several gigahertz and complete differential output signals with amplitude and phase imbalances less than $\pm$0.5 dB and $\pm$4°, respectively. These characteristics are particularly required for DC demodulation. Small insertion losses in the Tx portions, 1.0 and 1.2 dB for EGSM and DCS, respectively, were also obtained.**

***Index Terms*—Direct conversion (DC), dual band, front-end, global system for mobile communication (GSM), surface acoustic wave (SAW), SAW filter.**

I. Introduction

DIRECT-CONVERSION (DC) or low IF demodulation methods [1], [2] have been widely investigated for use in multiband cellular phones, such as the 900-MHz extended global system for mobile communications (EGSM), the 1.8-GHz digital cellular system (DCS), and 1.9-GHz personal communications system (PCS). Authors have already published switch-type surface-acoustic-wave (SAW) antenna duplexers, sometimes called SAW front-end modules (FEMs) for both dual- and triple-band transceivers [3], [4]. They can be used with heterodyne demodulation. However, requirements peculiar to DC demodulation have not been taken into consideration. Based on the blocking characteristics and spurious emission levels required for EGSM, DCS, and PCS [5], we have investigated configurations and the required performances for dual-band FEMs to be used with DC demodulation.

RF integrated circuits (RFICs) with DC demodulation generally have high spurious responses at harmonic frequencies, thus, attenuation levels of over 30–40-dB from the antenna port to the receiver (Rx) ports are needed up to several gigahertz. Recently, Rx low-noise amplifiers (LNAs) not only have been included in RFICs, but have also been operated differentially to reduce the effect of common-mode noise [1], [2]. For Rx LNAs to be included in RFICs, SAW filters with very low-loss characteristics are needed in the FEM to compensate for noise-figure degradation. For them to be operated differentially, complete differential Rx-output signals must be sent from the FEM. We have achieved low-loss characteristics in the Rx portions of the FEM with a new SAW filter. We have also achieved differential Rx-output ports with small amplitude and phase imbalances by developing lumped-element baluns. Moreover, we achieved high isolation characteristics from the transmitter (Tx) ports to Rx ports, making it possible to cut the number of switching p-i-n diodes in half, compared with conventional antenna switch modules [6]–[8]. The developed FEM is $8 \times 8 \times 1.85$ mm^3 and can be used with general RFICs using DC demodulation.

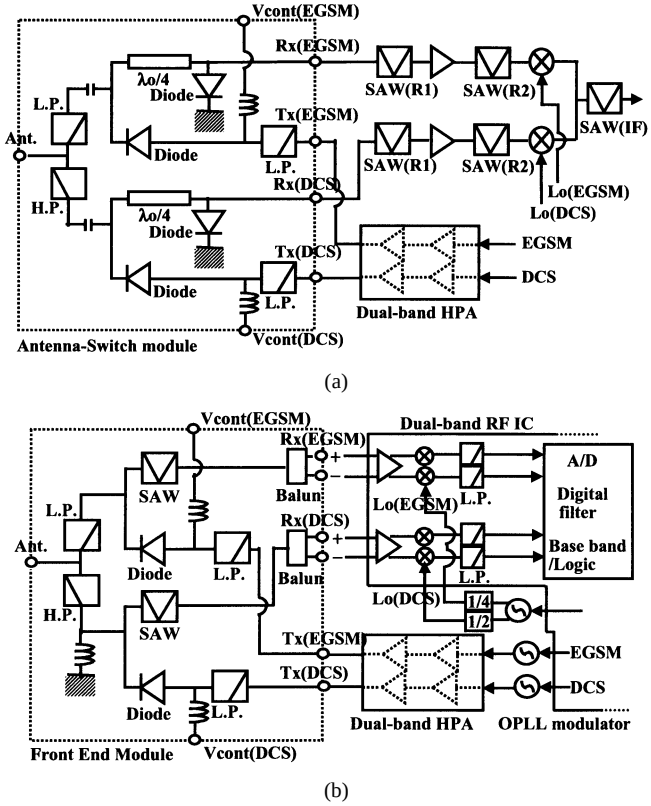

Fig. 1. Block diagram of a dual-band cellular-phone transceiver (900-MHz EGSM and 1.8-GHz DCS). (a) Conventional heterodyne-demodulation method; antenna-switch module is used. (b) DC demodulation method; SAW FEM is used.

Manuscript received October 16, 2001; revised February 13, 2002.

M. Hikita and N. Shibagaki are with the Central Research Laboratory, Hitachi Ltd., Tokyo 185-8601, Japan (e-mail: hikitami@crl.hitachi.co.jp).

N. Matsuura, K. Yokoyama, and K. Sakiyama are with Hitachi Media Electronics Ltd., Kanagawa 244-0817, Japan.

Digital Object Identifier 10.1109/TMTT.2002.804516

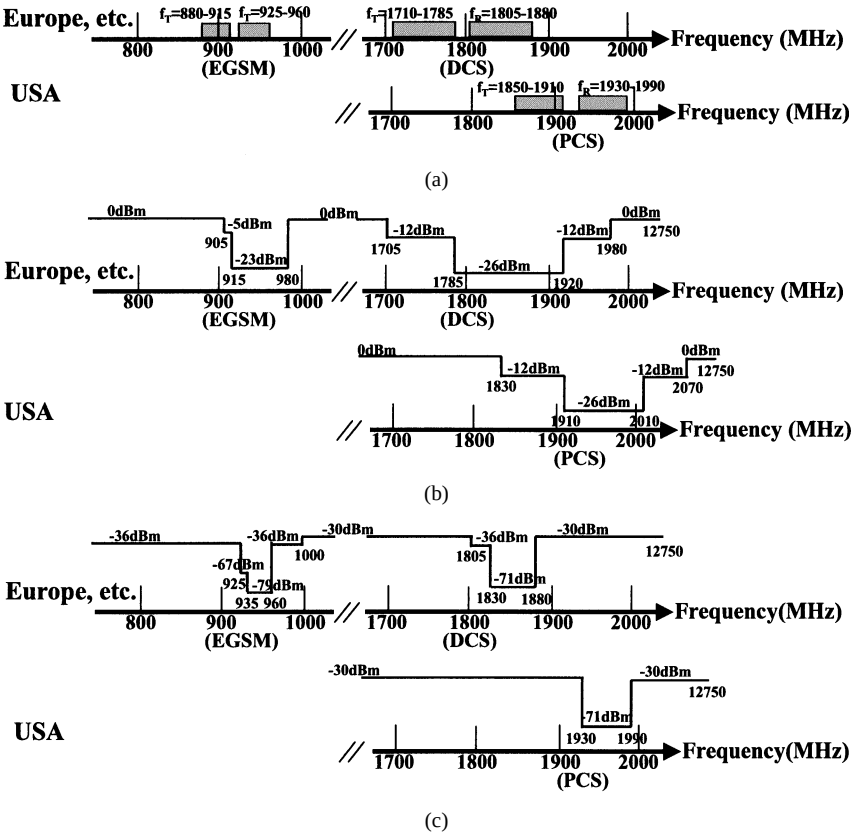

Fig. 2. System requirements for EGSM, DCS, and PCS from the Third Generation Partnership Project (3GPP) regulation [5]. (a) Frequency allocations. (b) Blocking characteristics. (c) Spurious emissions.

II. DC Transceiver for Global System for Mobile Communication (GSM)-Based Dual-Band Phones

A. Configuration

A block diagram of a conventional dual-band transceiver used in EGSM and DCS systems is illustrated in Fig. 1(a). Heterodyne demodulation is used, thus, inter-stage SAW filters (R2's) and an IF SAW filter are used between LNAs and mixs and after the mixs, respectively. Up-conversion is used to generate a Gaussian-filtered minimum shift-keying (GMSK) [5] modulated signal. A conventional antenna-switch module is also shown in Fig. 1(a) [6]–[8]. It not only switches between the transmitting and receiving states, but also separates 900-MHz and 1.8-GHz signals via a diplexer consisting of low-pass/high-pass filters. Four switching p-i-n diodes are used—two in the Tx portions and two in the Rx portions, as shown in Fig. 1(a).

A block diagram of our new dual-band transceiver using DC demodulation is shown in Fig. 1(b). The received signal is directly down-converted to baseband in- and quadrature-phase demodulated signals. This demodulation eliminates the need for the inter-stage R2 filters and the IF SAW filter, and simplifies the Rx-circuit configuration [1], [2]. A new FEM with SAW filters, the main focus of this paper, is also shown in this figure. Almost the same transceiver can be used in an EGSM/PCS dual-band transceiver.

The offset phase-locked-loop (OPLL) modulation method is now being used to generate GMSK signals, as shown in Fig. 1(b), which simplifies the Tx-circuit configuration drastically [9], [10]. This is because Tx voltage-controlled oscillators (VCOs) are directly modulated by baseband analog modulation signals from the OPLL circuit.

B. Requirements for Rx Portions of FEM

The frequency allocations for EGSM, DCS, and PCS are shown in Fig. 2(a). The frequency responses required for the Rx portions, i.e., paths from the antenna port to input ports of LNAs, are mainly determined by the blocking characteristics [5], which are shown in Fig. 2(b). RF filters are needed to protect LNAs and mixs from the blockers shown in Fig. 2(b). The attenuation levels in out-of-band are primarily determined by the difference between the blocker levels at the passband and those in the out-of-band as follows:

$$\text{Attenuation (Out-of-band)} \cong \text{Blocker (Out-of-band)} - \text{Blocker (Passband)}. \quad (1)$$

The characteristics required for EGSM, for example, are shown in Fig. 3.

RFICs with DC demodulation generally have high spurious responses at harmonic frequencies. This is because pseudolocal signals at frequencies of the local frequency multiplied by an odd-integer number are produced due to the saturated operation of the first mixs. Moreover, in a recent transceiver-circuit configuration [see Fig. 1(b)], the local signals for EGSM and DCS are generated by four- and two-time divisions, respectively, of the output signal from a single high-frequency VCO [2], which also produces pseudolocal signals at frequencies of the local frequency

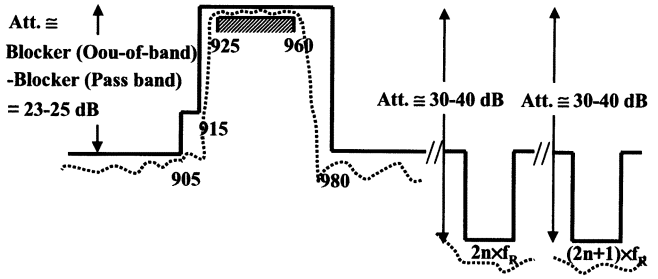

Fig. 3. Required frequency characteristics for the Rx portion of the FEM for EGSM.

multiplied by an even-integer number. These pseudolocal signals convert spurious signals at harmonic frequencies into noise-like baseband signals, which are very similar to the image-frequency responses of conventional heterodyne demodulation. Therefore, SAW filters in the FEM not only suppress the blockers of Fig. 2(b), but must also have high attenuation levels of 30–40 dB at harmonic frequencies. These levels are also shown in Fig. 3.

Recently, LNAs have been included in RFICs. In many cases, they are operated differentially to reduce the effect of the common-mode noise within the integrated circuits (ICs) [1], [2]. Therefore, not only the frequency characteristics of Fig. 3, but also complete differential Rx-output ports, are required for the FEM.

C. Requirements for Tx Portions of FEM

The frequency responses for the Tx portions, i.e., the paths from the output ports of a high-power amplifier (HPA) to an antenna port, are mainly determined by spurious emission characteristics [5], which are shown in Fig. 2(c). General HPAs have spurious emission levels from −35 to −40 dBc at harmonic frequencies [11]. Therefore, though passband insertion losses in the Tx portions must be as small as possible, the attenuation levels at harmonic frequencies must be 30–35 dB. Particularly for the EGSM-Tx portion, where twice the transmitted frequency $2f_T(\mathrm{EGSM})$ overlaps the DCS received frequency $f_R(\mathrm{DCS})$, the attenuation levels must be 35–40 dB. These required characteristics are shown in Fig. 4(a) and (b) for EGSM and DCS, respectively.

Except for the EGSM second harmonic signal going through the main path of the EGSM-Tx portion of the FEM, two more things must be considered. One is the EGSM second harmonic signal coming from the DCS output port of the dual-band HPA and entering the DCS-Tx input port. The generated harmonic signal is partially transferred from EGSM matching circuits to DCS matching circuits within the dual-band HPA. It goes through the DCS-Tx portion of the FEM and is emitted from the antenna. Large spurious emissions occur if this signal is coherently added to the EGSM second harmonic signal coming from the main path of the EGSM-Tx portion. The coupling from the EGSM circuits to the DCS circuits within the HPA is approximately −20 dB [11], which means that the attenuation level in the DCS-Tx portion in the off state must be 25–30 dB. This is also shown in Fig. 4(b).

The other thing to consider is the nonlinearity of the switching elements. The switching p-i-n diodes of Fig. 1(b) have nonlinear characteristics in the off state, which generate harmonic-frequency signals. These signals must be kept as small as possible. Under full-transmitting-power conditions, i.e., 35 dBm for EGSM and 32 dBm for DCS [5], the emission power due to the nonlinearity of the p-i-n diodes must be from −50 to −40 dBm

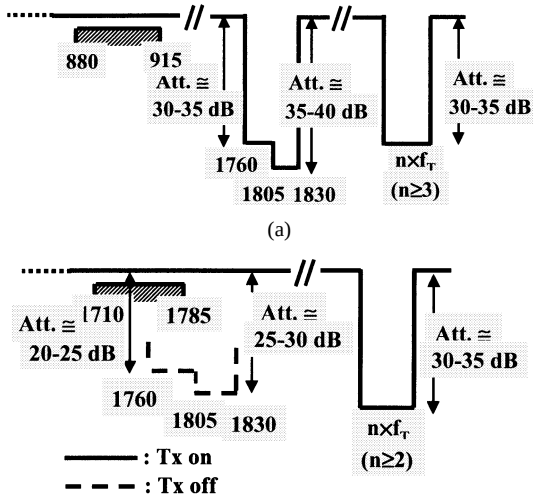

Fig. 4. Required frequency characteristics for Tx portions of the FEM. (a) Tx portion of EGSM; 1805–1830-MHz overlaps $f_R(\mathrm{DCS})$. (b) The Tx portion of the DCS; spurious signal at $2f_T(\mathrm{EGSM})$ must be suppressed in the EGSM-Tx on state (DCS-Tx off state).

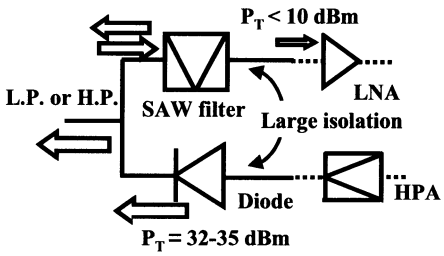

Fig. 5. Switchless structure for Rx portions. The SAW filter and p-i-n diode are directly connected in parallel.

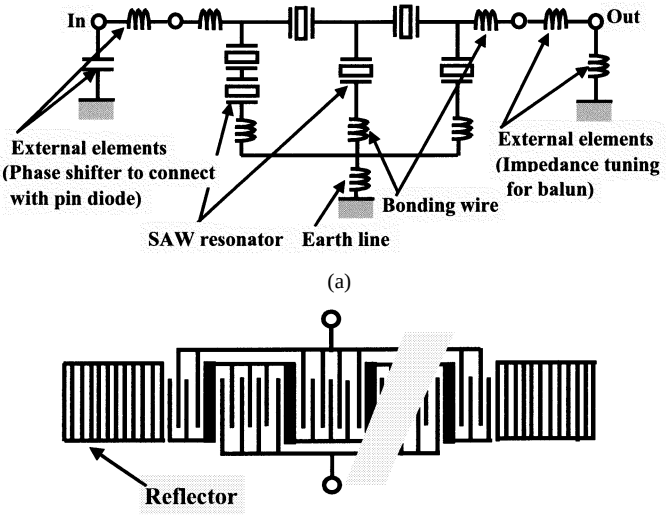

Fig. 6. Rx SAW filter with high-power and sharp-cutoff frequency characteristics. (a) SAW-resonator-coupled filter, i.e., ladder-type configuration. (b) Electrically connected multi-IDT SAW resonator.

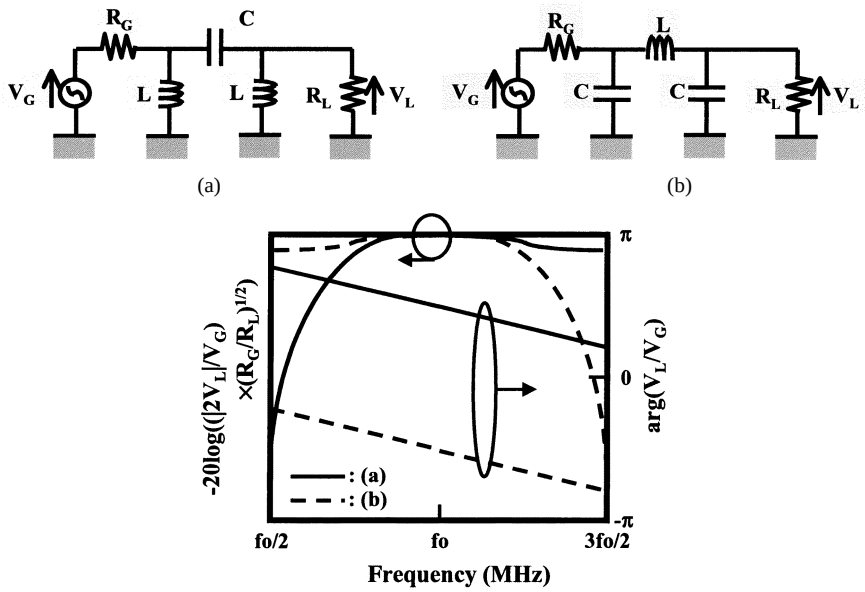

Fig. 7. Π-type impedance transformer circuits. (a) Circuit with phase from π to 0 for frequency from 0 to ∞. (b) Circuit with phase from 0 to $-\pi$ for frequency from 0 to ∞. (c) Amplitude and phase relations of (a) and (b).

at the antenna port of the FEM. We investigated adding a supplementary circuit to the p-i-n diode to achieve these requirements. This circuit will be described later.

III. New Receiver Portions Including SAW Filters

A. Simple Switchless Structure

To simplify the circuits for the Rx portions, we used the new switchless structure shown in Fig. 5. The maximum power input to conventional LNAs in the off state must be less than 10 dBm, which requires isolation characteristics of over 25 dB at the f_Ts between the output ports of the HPA and the input ports of the LNAs. We achieved the almost all required isolation level only by SAW filters using the SAW-resonator-coupled filters [12], i.e., one of a ladder-type configuration shown in Fig. 6(a). While keeping low-loss characteristics, we can design very sharp cutoff frequency responses by combining electrically connected multi-inter-digital transducer (IDT) SAW resonators shown in Fig. 6(b) [12]. This is very important because both EGSM and DCS have very wide bandwidths for the frequencies transmitted (f_Ts) and the frequencies received (f_Rs), but the relative spacing bandwidths between them are very narrow, as shown in Fig. 2(a).

We have developed a direct-parallel connection between the SAW filters and the switching p-i-n diodes, as shown in Fig. 5, eliminating the need for p-i-n diodes in the Rx portions of the FEM, as shown in Fig. 1(b). These parallel connections require SAW filters that have not only high attenuation levels, but also high-impedance characteristics at the f_Ts. This is because to minimize the increase in the losses in the Tx portions due to the parallel connections, the input impedance of the parallel-connected sides of the SAW filters must be designed as large as possible at the f_Ts. Moreover, the SAW filters must have very high-power-handling capabilities and small nonlinear characteristics to protect against the high transmitted power, i.e., 35 and 32 dBm, entering from the Tx portions.

We achieved the required characteristics by using the previously published SAW filter design procedures for the ladder-type configuration. The equivalent circuit is shown in Fig. 6(a), and the SAW resonators are shown in Fig. 6(b) [12]. The external elements on the parallel-connected side (left-hand side) act as a phase shifter and make the impedance of the SAW filter as high as possible at the f_T. The role of the external elements on the Rx side (right-hand side) is impedance tuning for the balun, which will be described later. The electrically connected multi-IDT SAW resonators have intrinsically high-power durability characteristics because of their fourfold larger apertures compared with those of conventional multifinger IDT-type resonators with the same impedance [12]. Furthermore, two SAW resonators connected serially are arranged as shunt-arm elements at the parallel-connected side within the filter of Fig. 6(a), which further increases power durability. We have already conducted a power-accelerated aging test over several hundred hours with an input power of 10 W at the f_T for EGSM and of 5 W at the f_T for DCS.

B. Differential Output Ports

There are several ways to obtain differential-output signals from a SAW filter. The use of an inter-digitated inter-digital transducer (IIDT) transversal SAW filter having one input and two outputs with opposite phases is a common way to obtain differential-output signals from a SAW filter [13]–[15]. However, the power-handling capability of transversal filters is small, and the designed differential-output impedance is restricted. Moreover, from our fundamental investigation and experiment, the conventional SAW filter could not satisfy the system requirements from recent RFICs (amplitude and phase imbalances less than ± 1 dB and $\pm 10^\circ$, respectively, as explained in V).

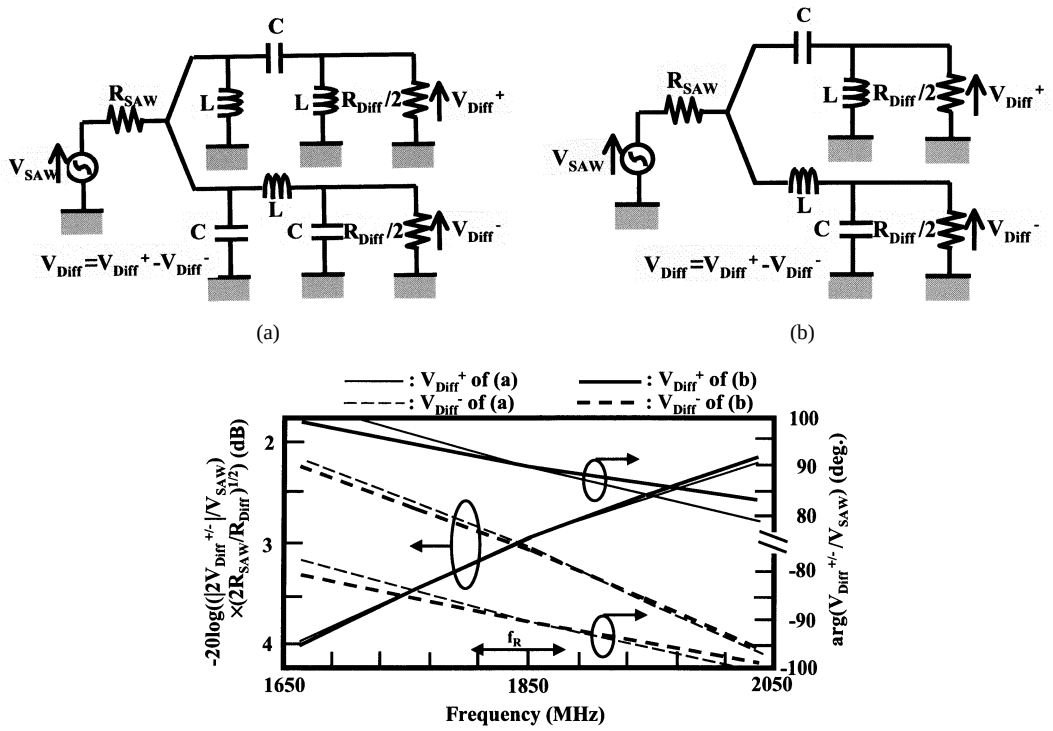

Fig. 8. Lumped-element baluns and examples of frequency characteristics. (a) Balun with π-type circuits. (b) Balun with simplified π-type circuits. (c) Simulation results for DCS.

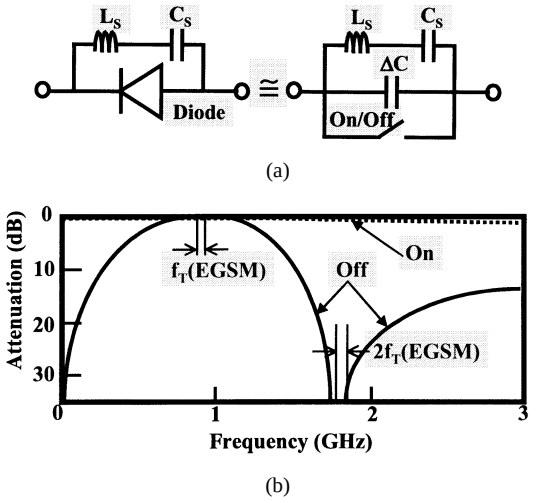

Fig. 9. Techniques for reducing second harmonic generation characteristics and achieving high attenuation in the off state for a DCS-Tx p-i-n diode. (a) Addition of serial-connected L_S and C_S to a p-i-n diode in parallel. L_S and C_S are not only resonated at $f_T(\mathrm{EGSM})$, but are also antiresonated with ΔC at $2\,f_T(\mathrm{EGSM})$. (b) Frequency characteristics of (a).

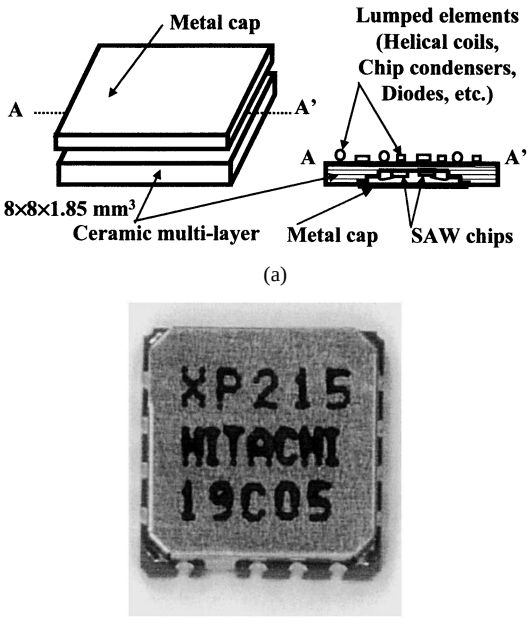

Fig. 10. Developed EGSM/DCS dual-band FEM. (a) Module structure. (b) Photograph of the FEM.

To achieve a differential-output impedance with any value as well as good amplitude- and phase-balanced characteristics, we have developed a lumped-element balun consisting of two π-type impedance-transformer circuits. As shown in Fig. 7(a) and (b), two types of impedance-transformer circuits are possible. When $L/C = R_G R_L$ is achieved, impedance transformation from R_G to R_L or vice versa can be realized near resonant frequency fo$(= 1/(2\pi(LC)^{1/2}))$ with either circuit. The amplitude and phase relations of the transfer functions between $V_G s$ and $V_L s$ are given by

$$\text{Amp.} = -20\log\left(\left(|2V_L|/V_G\right)\left(R_G/R_L\right)^{1/2}\right) \tag{2a}$$

$$\text{Phase} = \arg\left(V_L/V_G\right). \tag{2b}$$

They are also schematically shown in Fig. 7(c). Almost identical amplitude characteristics and phases of approximately $\pi/2$ with

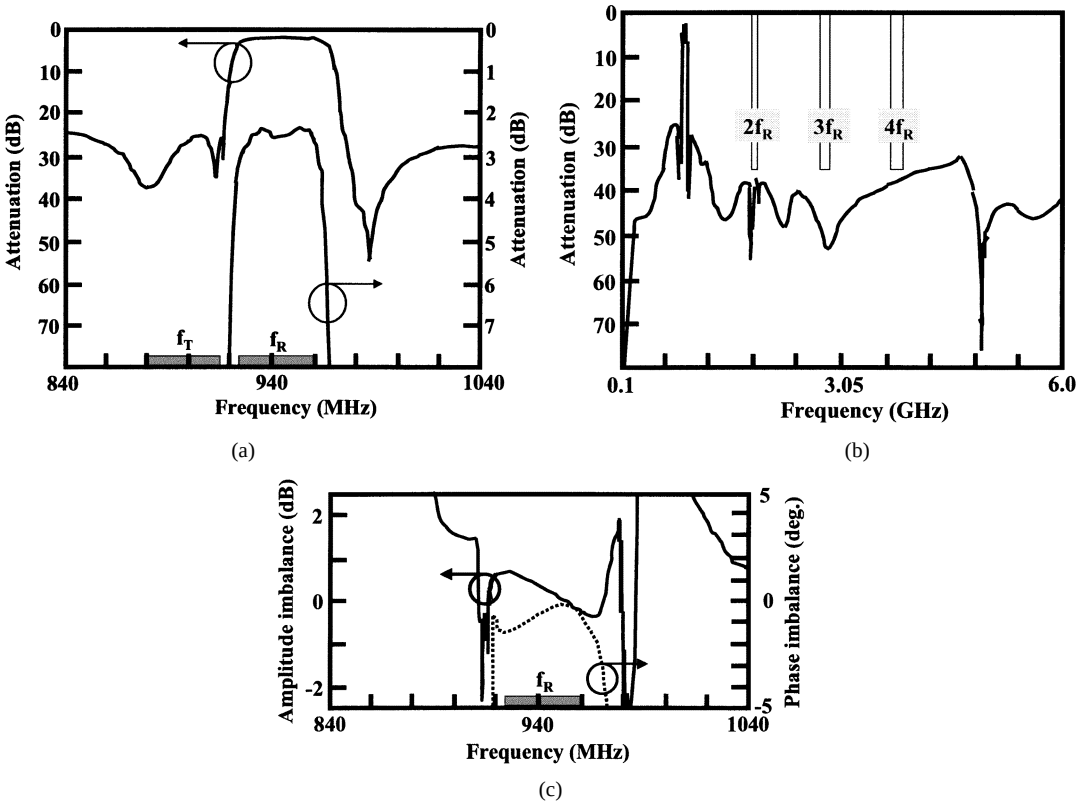

Fig. 11. Frequency characteristics for the EGSM-Rx portion of the FEM. (a) Passband characteristics. (b) Out-of-band characteristics. (c) Amplitude- and phase-imbalance characteristics.

opposite signs between the two types of circuits [see Fig. 7(a) and (b)] are obtained near fo.

To make a balun circuit, we connected the input ports of the two types of circuits in parallel, as shown in Fig. 8(a). L and C are resonated near fo, which makes it possible to transform the circuit of Fig. 8(a) into the simplified one of Fig. 8(b). The output impedance of the SAW filter ($R_{\rm SAW}$) and the differential impedance of the RFIC ($R_{\rm Diff}$) are related to L and C as follows:

$$L = \left(R_{\rm SAW}R_{\rm Diff}\right)^{1/2}/(2\pi {\rm fo}) \tag{3a}$$

$$C = \left(R_{\rm SAW}R_{\rm Diff}\right)^{-1/2}/(2\pi {\rm fo}). \tag{3b}$$

The computer-simulated amplitudes and phases of the designed balun, e.g., for DCS, are shown in Fig. 8(c). We show the DCS results because DCS has the widest bandwidth of the cellular systems currently in use. The parameters used in the simulation were

$$R_{\rm SAW} = 50\,\Omega \tag{4a}$$

$$R_{\rm Diff} = 100\,\Omega \tag{4b}$$

$$L = 6.1079\ {\rm nH} \tag{5a}$$

$$C = 1.2216\ {\rm pF}. \tag{5b}$$

The amplitude and phase relations of the transfer functions between $V_{\rm SAW}$ and the output voltages $V_{\rm Diff}^{+}$ and $V_{\rm Diff}^{-}$ are

$${\rm Amp.}^{+/-} = -20\log\left(\left(|2V_{\rm Diff}^{+/-}|/V_{\rm SAW}\right)\left(2R_{\rm SAW}/R_{\rm Diff}\right)^{1/2}\right) \tag{6a}$$

$${\rm Phase}^{+/-} = \arg\left(V_{\rm Diff}^{+/-}/V_{\rm SAW}\right). \tag{6b}$$

The comparison of the characteristics of the normal π-type balun [see Fig. 8(a)] and the simple π-type balun [see Fig. 8(b)] shown in Fig. 8(c) indicates that almost the same performance can be achieved with both types of baluns. The amplitude and phase imbalances between the differential output voltages are defined as

$$\Delta{\rm Amp.} = {\rm Amp.}^{-} - {\rm Amp.}^{+} \tag{7a}$$

$$\Delta{\rm Phase} = 180^\circ - \left({\rm Phase}^{-} - {\rm Phase}^{+}\right). \tag{7b}$$

The simulation results indicate that an amplitude imbalance less than ± 0.25 dB and a phase imbalance less than $\pm 3^\circ$ can be achieved in the passband, even for the widest system of DCS. Very accurate values with minute deviations are required for L and C, as given by (5a) and (5b). In general, $R_{\rm Diff}$ depends on the RFIC used. However, $R_{\rm SAW}$ can be changed by adding tuning circuits. The external elements on the Rx side of the equivalent circuit of Fig. 6(a) show such circuits. As shown by (3a) and (3b), more realistic values for L and C can be obtained by slightly changing $R_{\rm SAW}$ using the tuning elements. The experimental data will be presented later.

IV. Improved Trasmitter Portions

The most important characteristics required for the Tx portions are low-insertion losses at the passbands and high-attenuation characteristics at harmonic frequencies. The nonlinearity of a switching p-i-n diode in the Tx off state should also be considered, which requires a supplementary circuit specifically for

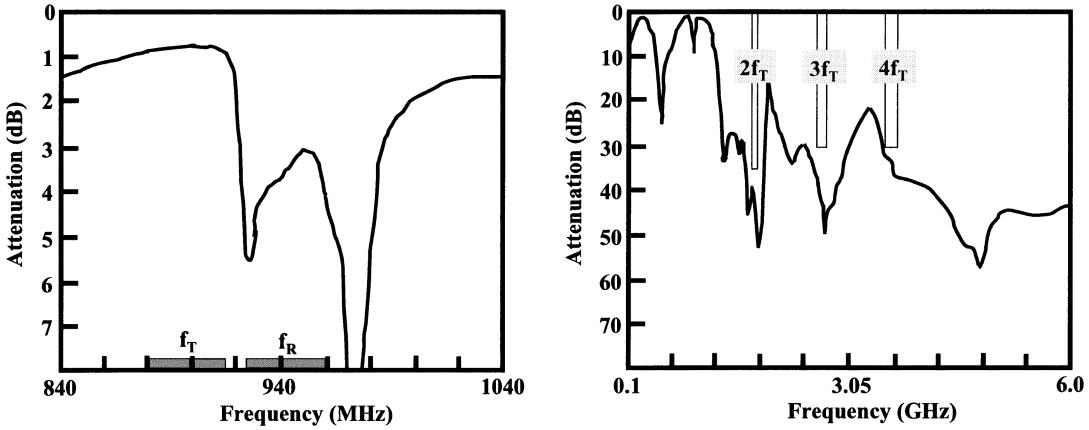

(a) (b)

Fig. 12. Frequency characteristics for the EGSM-Tx portion of the FEM. (a) Passband characteristics. (b) Out-of-band characteristics.

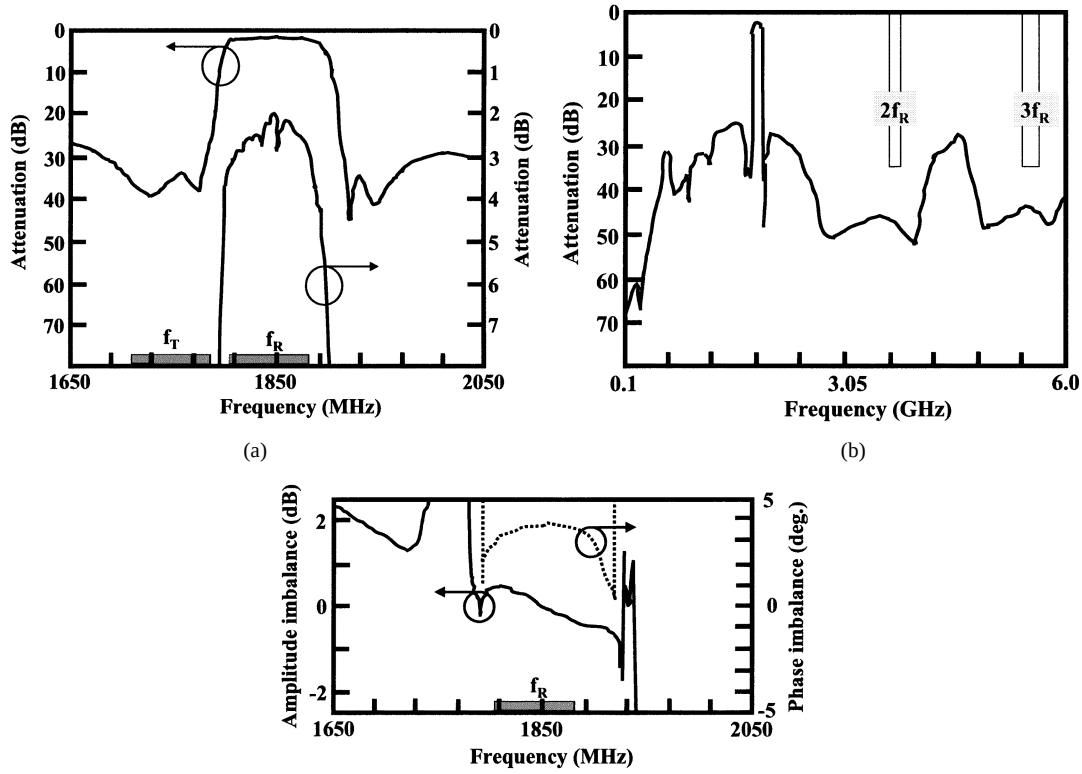

(a) (b) (b)

Fig. 13. Frequency characteristics for the DCS-Rx portion of the FEM. (a) Passband characteristics. (b) Out-of-band characteristics. (c) Amplitude- and phase-imbalance characteristics.

the diode of the DCS-Tx portion. To reduce the strength of the second harmonic signal generated from the DCS-Tx diode, we added a circuit consisting of serial-connected L_S and C_S to the p-i-n diode in parallel, as shown in Fig. 9(a). These L_S and C_S are resonated at the $f_T(\mathrm{EGSM})$. A very low impedance can be obtained at the resonant frequency, which reduces the voltage difference between the input and output ports of the p-i-n diode against the high EGSM transmitted power of 35 dBm. Very small second harmonic generation characteristics were achieved with this circuit configuration. The experimental data will be presented later.

A p-i-n diode is equivalently represented by a small capacitance ΔC and an ideal switch connected in parallel, as shown in Fig. 9(a), together with L_S and C_S. The circuit of serial-connected L_S and C_S is resonated with ΔC at $2f_T(\mathrm{EGSM})$, which leads to very a high impedance in the DCS-Tx off state. Due to this high impedance, the required high attenuation levels at $2f_T(\mathrm{EGSM})$ can be realized in the off state. A schematic illustration of the frequency characteristics between the input and output ports of Fig. 9(a) is shown in Fig. 9(b), which corresponds to the requirements of Fig. 4(b).

The attenuation levels required at the harmonic frequencies given in Fig. 4(a) and (b) for the EGSM- and DCS-Tx on states were achieved using conventional low-pass filter design techniques. The experimental characteristics of the designed results will be presented below.

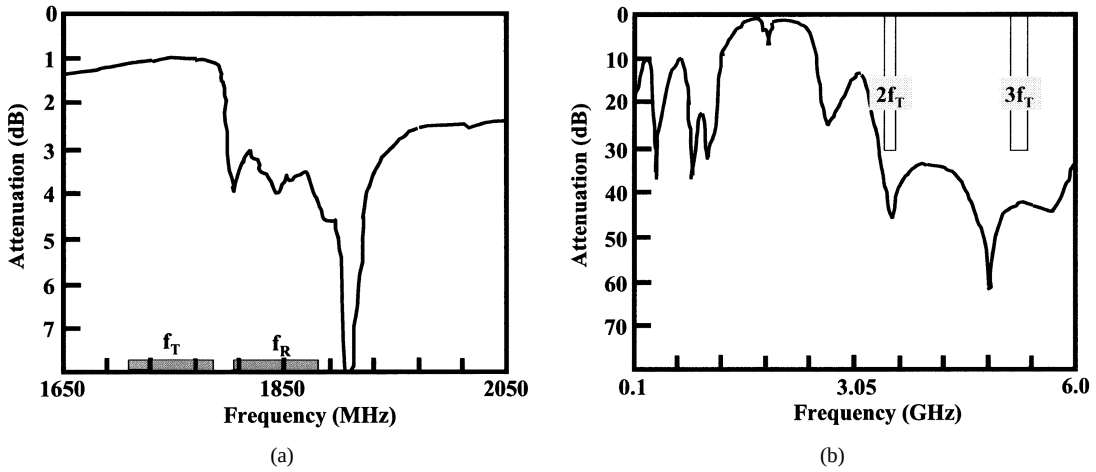

Fig. 14. Frequency characteristics for the DCS-Tx portion of the FEM. (a) Passband characteristics. (b) Out-of-band characteristics.

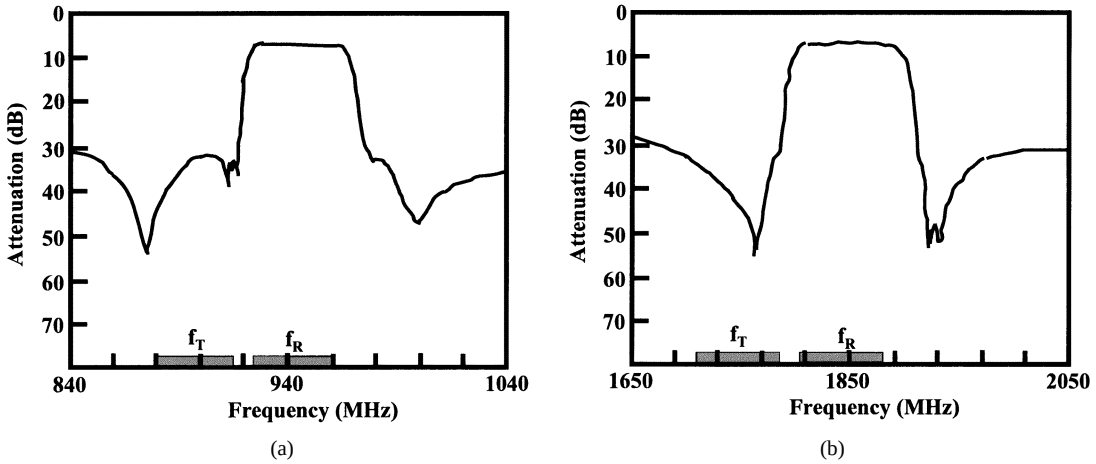

Fig. 15. Isolation characteristics between Tx-input and Rx-output ports of the FEM in the Tx on state. (a) EGSM portion. (b) DCS portion.

V. Experimental Results

We developed an FEM for use in an EGSM/DCS dual-band transceiver using DC demodulation. A ceramic multilayer package and lumped-circuit elements were used, as shown in Fig. 10(a). Other dual-band FEMs, e.g., EGSM/PCS, are also possible using the same technologies. SAW chips were mounted in a pocket on the lower side of the package. Approximately 70% of the circuits were made of lumped elements, i.e., miniature helical inductors and chip condensers, mounted on the upper side of the package. We formed the remaining circuits using internal elements with thin ceramic layers. The baluns to transform the single-ended output port of the SAW filter into the differential output ports were made of lumped elements. A diplexer consisting of low-pass/high-pass filters was also made of lumped elements. The low-pass filters used in the Tx portions to suppress spurious signals at harmonic frequencies were formed mainly of internal elements.

We used a conventional $LiTaO_3$ piezoelectric substrate, i.e., 36°–42°-rotated Y-cut X-propagation $LiTaO_3$ [16]–[18], for the SAW filters. The developed FEM was $8 \times 8 \times 1.85$ mm^3; a photograph of it is shown in Fig. 10(b). The control voltage and current value for switching were 2.5 V and approximately 6 mA, respectively, for each p-i-n diode in the on state.

The frequency characteristics of the EGSM-Rx portion of the FEM, i.e., the characteristics from the antenna port to the EGSM-Rx ports, are shown in Fig. 11(a)–(c). The antenna port had 50-Ω single-ended input impedance, while the Rx ports had 100-Ω differential output impedance between them. As shown in Fig. 11(a) and (b), the insertion loss was 3.0 dB, and sharp-cutoff frequency characteristics and sufficient attenuation levels against blockers were achieved. High suppression characteristics at harmonic frequencies over 35 dB were also obtained, which is required for DC demodulation. Amplitude and phase imbalances less than ±0.4 dB and ±3°, respectively, were achieved, as shown in Fig. (c). These balanced characteristics were achieved using general lumped-element chip condensers and helical inductors without any trimming or tuning. Recent RFICs using DC demodulation strongly require amplitude and phase imbalances less than ±1 dB and ±10°, respectively.

The frequency characteristics of the EGSM-Tx portion of the FEM, i.e., the characteristics from the Tx to antenna ports, are shown in Fig. 12(a) and (b), where both ports had the 50-Ω single-ended impedance. An insertion loss as small as 1.0 dB and a suppression level over 35 dB at the second harmonic frequency were achieved. The suppression levels at the third and fourth harmonic frequencies were over 30 dB.

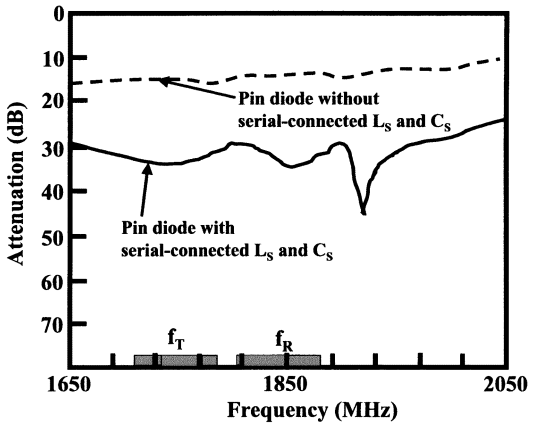

Fig. 16. Attenuation characteristics for the DCS-Tx portion of the FEM in the DCS-Tx off state. Serial-connected L_S and C_S are antiresonated with ΔC of an off-state p-i-n diode.

The frequency characteristics of the DCS-Rx portion are shown in Fig. 13(a)–(c), where the Rx ports also had 100-Ω differential output impedance. The insertion loss was 3.3 dB, and sufficient suppression levels against blockers were achieved. High-suppression characteristics at harmonic frequencies over 35 dB were obtained. The amplitude and phase imbalances were less than ± 0.5 dB and $\pm 4^\circ$, respectively. These balanced characteristics were achieved using the same kinds of general chip condensers and helical inductors as used in the EGSM-Rx portion. The frequency characteristics of the DCS-Tx portion are shown in Fig. 14(a) and (b). The insertion loss was as small as 1.2 dB, and the suppression levels at the second and third harmonic frequencies were over 30 dB.

The isolation characteristics between the Tx-input and Rx-output ports in EGSM- and DCS-Tx on states are shown in Fig. 15(a) and (b), respectively. Isolation levels over 30 dB at the $f_T s$ were achieved, which eliminates the need for p-i-n diodes in the Rx portions of the FEM.

The attenuation characteristics of the DCS-Tx portion in the DCS-Tx off state are shown in Fig. 16. We conducted two experiments. In one, we used a p-i-n diode without serial-connected L_S and C_S. In the other, we used a p-i-n diode with serial-connected L_S and C_S, as shown in Fig. 9(a). We achieved approximately 15-dB attenuation improvement with the latter configuration compared with the former, and the requirements of Fig. 4(b) are satisfied.

The second harmonic generation characteristics of the DCS-Tx portion in the EGSM-Tx on state, i.e., the DCS-Tx off state, are shown in Fig. 17(a). We again conducted two experiments, corresponding to the above two. We achieved second harmonic levels less than -50 dBm with the latter configuration even for 35-dBm EGSM transmitted power. These values are 15–20 dB smaller than those with the former configuration, as shown in Fig. 17(a).

Power-compression phenomena were also observed due to nonlinearity or the saturation characteristics of the p-i-n diode in the on state. The relationship between the input power at the Tx-input port and the output power at the antenna port is shown in Fig. 17(b), taking EGSM as an example. A very large 1-dB output-power compression point of 39 dBm was achieved. This level is sufficient for cellular-phone use.

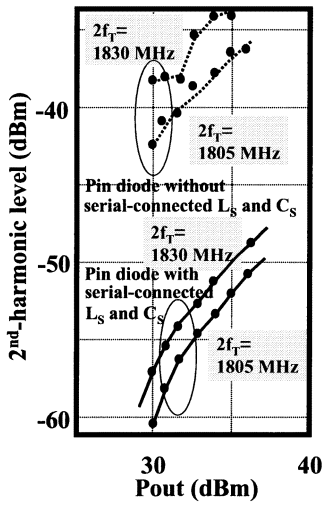

(a)

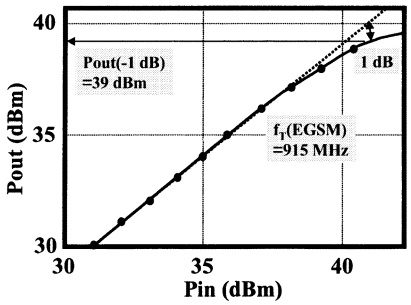

(b)

Fig. 17. Characteristics of the FEM for high transmitted power. Examples of the EGSM are shown. (a) Resonance of serial-connected L_S and C_S reduced second harmonic generation. (b) Power compression, i.e., $P_{\rm in}$ versus $P{\rm out}$.

VI. Conclusion

1) Assuming DC demodulation, we have investigated and proposed new configurations for the SAW FEMs used in GSM-based dual-band cellular-phone transceivers.
2) A direct-parallel connection between the SAW filters and the switching p-i-n diodes has been developed, which could eliminate the need for diodes in the Rx portions of the FEMs.
3) The design procedures for high-power SAW filters, differential Rx-output ports, and the improved Tx portion of the FEMs have also been presented.
4) The developed EGSM/DCS dual-band FEM, which is $8 \times 8 \times 1.85$ mm^3 and satisfies the system specifications can be used with RFICs using DC demodulation and general dual-band HPAs.

References

[1] J. Strange and S. Atkinson, "A direct conversion transceiver for multi-band GSM application," in *Proc. IEEE Radio Freq. Integrated Circuits Symp.*, 2000, pp. 25–28.

[2] *RF Transceiver IC for GSM900/1800 Dual Band Cellular Systems RF IC Catalog*, Hitachi Ltd., Tokyo, Japan, 2001.

[3] M. Hikita, N. Matsuura, N. Shibagaki, and K. Sakiyama, "New SAW antenna duplexers for single- and dual-band handy phones used in 800-MHz and 1.8-GHz cellular-radio systems," in *Proc. IEEE Ultrason. Symp.*, 1999, pp. 385–388.
[4] N. Shibagaki, N. Matsuura, K. Sakiyama, and M. Hikita, "An integrated SAW antenna duplexer for EGSM/DCS1800/PCS triple-band cellular systems," in *Proc. IEEE Ultrason. Symp.*, 2000, pp. 391–394.
[5] "3rd Generation Partnership Project," Tech. Specification Group, GSM/EDGE (3GPP TS 05.05), V8.9, 2001.
[6] T. Watanabe, K. Furutani, N. Nakajima, and H. Mandai, "Antenna switch duplexer for dualband phone (GSM/DCS) using LTCC multilayer technology," in *IEEE MTT-S Int. Microwave Symp. Dig.*, 1999, pp. 215–218.
[7] F. Uchikoba, T. Goi, N. Harada, and S. Nakai, "Multi-chip module with bare SAW device," in *Proc. Int. Acoustic Wave Devices for Future Mobile Commun. Syst. Symp.*, Chiba , Japan, Mar. 2001, pp. 145–150.
[8] R. Lucero, W. Qutteneh, A. Pavio, D. Meyers, and J. Estes, "Design of an LTCC switch diplexer front-end module for GSM/DCS/PCS applications," in *Proc. IEEE Radio Freq. Integrated Circuits Symp.*, 2001, pp. 213–216.
[9] T. Yamawaki, M. Kokubo, K. Irie, H. Matsui, K. Hori, T. Endou, H. Hagisawa, T. Furuya, Y. Shimizu, M. Katagishi, and J. R. Hildersley, "A 2.7-V GSM RF transceiver IC," *IEEE J. Solid-State Circuits*, vol. 32, pp. 2089–2096, Dec. 1997.
[10] RF Micro Devices, "Reduced filter requirements using an ultra low noise modulator," *Microwave J.*, pp. 200–214, Jan. 2001.
[11] *MOS FET Power Amplifier Module for E-GSM and DCS 1800 Dual Band Handy Phone, Power Module Catalog*, Hitachi Ltd., Tokyo, Japan, 2000.
[12] M. Hikita, N. Shibagaki, K. Sakiyama, and K. Hasegawa, "Design methodology and experimental results for new ladder-type SAW resonator coupled filters," *IEEE Trans. Ultrason., Ferroelect., Freq. Contr.*, vol. 42, pp. 495–508, July 1995.
[13] G. Endoh, M. Ueda, O. Kawachi, and Y. Fujiwara, "High performance balanced type SAW filters in the range of 900 MHz and 1.9 GHz," in *Proc. IEEE Ultrason. Symp.*, 1997, pp. 41–44.
[14] H. Meier, T. Baier, and G. Riha, "Miniaturization and advanced functionalities of SAW devices," in *Proc. IEEE Ultrason. Symp.*, 2000, pp. 395–400.
[15] M. Koshino, K. Kanasaki, N. Akahori, M. Kawase, R. Chujyo, and Y. Ebata, "A wide-band balanced SAW filter with longitudinal multi-mode resonator," in *Proc. IEEE Ultrason. Symp.*, 2000, pp. 387–390.
[16] N. Nakamura, M. Kazumi, and H. Shimizu, "SH-type and Rayleigh-type surface wave on rotated Y-cu $LiTaO_3$," in *Proc. IEEE Ultrason. Symp.*, 1977, pp. 819–822.
[17] M. Hikita, A. Isobe, A. Sumioka, N. Matsuura, and K. Okazaki, "Rigorous treatment of leaky SAWs and new equivalent circuit representation for interdigital transducers," *IEEE Trans. Ultrason., Ferroelect., Freq. Contr.*, vol. 43, pp. 482–490, May 1996.
[18] K. Hashimoto, M. Yamaguchi, S. Mineyoshi, O. Kawachi, M. Ueda, G. Endoh, and O. Ikata, "Optimum leaky-SAW cut of $LiTaO_3$ for minimized insertion loss devices," in *Proc. IEEE Ultrason. Symp.*, 1997, pp. 245–254.

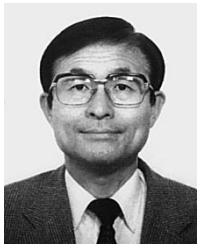

Mitsutaka Hikita (M'88–SM'94–F'02) received the B.S., M.S., and Ph.D. degrees in electronics engineering from Hokkaido University, Sapporo, Japan, in 1972, 1974 and 1977, respectively.

From 1972 to 1978, he was engaged in analysis of electromagnetic-field problems, microwave acoustics, and acoustic-optic interactions. In 1978, he joined the Central Research Laboratory, Hitachi Ltd., Tokyo, Japan. From 1978 to 1987, he was involved with high-performance RF SAW filters. From 1987 to 1994, he was involved with microwave devices for space communications, timing-extraction high-Q SAW resonators for optical communications, and SAW duplexer. From 1994 to 1999, he was a leader of the RF Si-IC and SAW Technology Group. In 1998, he became a Chief Researcher and was recently engaged in RF circuit design for cellular phones and advanced applications of SAW technologies.

Dr. Hikita is a member of the Institute of Electronics, Information and Communication Engineers (IEICE), Japan. He was the recipient of the 1990 IEEE Microwave Theory and Techniques Society (IEEE MTT-S) Microwave Prize Award, the 1991 Invention Award presented by the Invention Association of Japan, and the 1993 Science and Technology Agency of Japan Award of Commendation presented by the Minister of State for Science and Technology.

Naoki Matsuura graduated from Kanazawa University, Ishikawa, Japan, in 1993.

In 1993, he joined Hitachi Hi-Techno Ltd., Kanagawa, Japan. In 1995, he joined Hitachi Media Electronics Ltd., Kanagawa, Japan. Since 1993, he has been engaged in research and development on RF circuits and SAW devices for mobile communications.

Mr. Matsuura is a member of the Institute of Electronics, Information and Communication Engineers (IEICE) of Japan.

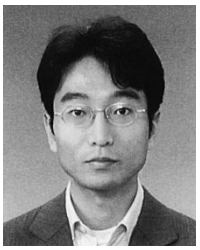

Kazuyuki Yokoyama graduated from Takayama Industrial High School, Takayama, Japan, in 1992.

In 1992, he joined Hitachi Media Electronics Ltd., Yokohama, Japan, where he has been engaged in the development of television tuners and design of RF circuits for mobile communications.

Mr. Yokoyama is a member of the Institute of Electronics, Information and Communication Engineers (IEICE), Japan.

Nobuhiko Shibagaki received the B.S. and M.S. degrees in material engineering from the Nagoya Institute of Technology, Nagoya, Japan, in 1985 and 1987, respectively.

In 1987, he joined the Central Research Laboratory, Hitachi Ltd., Tokyo, Japan, where he has been engaged in research and development of SAW devices for mobile communications, especially SAW duplexers for cellular phones and SAW FEMs for GSM-based handy phones.

Mr. Shibagaki is a member of the Institute of Electronics, Information and Communication Engineers (IEICE), Japan.

Kazuyuki Sakiyama received the B.S. and M.S. degrees in applied physics from Tohoku University, Sendai, Japan, in 1976 and 1978, respectively.

In 1978, he joined Yokohama Works, Hitachi Ltd., Yokohama, Japan. In 1997, he joined Hitachi Media Electronics Ltd., Yokohama, Japan, where he has been involved with SAW-material investigation and process-technology development. He has recently been engaged in the design and development of SAW devices, especially SAW FEMs for GSM-based handy phones.

Mr. Sakiyama is a member of the Institute of Electronics, Information and Communication Engineers (IEICE), Japan.